

Magneto-optical studies of organic electroluminescent materials having fast reverse intersystem crossing

Xin Pan^{1,*}, Dipak Raj Khanal,¹ Ohyun Kwon^{2,†}, and Zeev Valy Vardeny^{1,‡}

¹*Department of Physics & Astronomy, University of Utah, 115 South 1400 East, Salt Lake City, Utah, 84112 USA*

²*Samsung Advanced Institute of Technology, Samsung Electronics Co., Ltd., 130, Samsung-Ro, Youngtong-Gu, Suwon-Si, Gyeonggi-do 16678, Republic of Korea*



(Received 30 August 2023; revised 3 March 2024; accepted 12 March 2024; published 27 March 2024)

In thermally activated delayed-fluorescence (TADF) materials, the fluorescence efficiency is enhanced through reverse intersystem crossing (RISC) from triplet to singlet excitons. The performance of organic light-emitting devices (OLEDs) based on TADF materials highly depends on the thermal conversion efficiency of the lowest triplet exciton T_1 into the lowest singlet exciton S_1 , which relates to the energy difference $\Delta E_{S_1-T_1}$. Here we investigate the RISC process in two TADF compounds with vastly different $\Delta E_{S_1-T_1}$ using magneto-optical spectroscopies that include magnetophotoinduced absorption (MPA) in films and magnetoelctroluminescence (MEL) in OLEDs. The photoinduced absorption spectrum of the fast RISC material clearly shows that both singlet and triplet excitons coexist under steady-state conditions. Since the MPA response of the singlet and triplet excitons are similar and have the same polarity, we conclude that the magnetic field does not influence the RISC process in the studied compounds. We also find that the MEL response in OLEDs based on these compounds originates from the injected polaron pair species before they decay into S_1 and T_1 excitonic states in the emissive TADF layer.

DOI: 10.1103/PhysRevApplied.21.034057

I. INTRODUCTION

In organic light-emitting devices (OLEDs) the spin statistics dictates that excitons in the emission layer that are generated from the injected positive and negative polarons (P^+ and P^-) from the opposite electrodes are formed in a ratio of 1:3 of singlet and triplet spin states. This limitation means that for OLEDs based on fluorescent materials, the internal quantum efficiency (IQE) can reach a maximum value of only 25% when accounting for radiative recombination only in the singlet configurations. In order to harvest the generated triplet states in the emissive layer, a successful method is the use of thermally activated delayed-fluorescence (TADF) compounds [1–7]. These compounds show thermal conversion of the triplet states into singlet states, known as “reverse-intersystem crossing” (RISC) [see Fig. 1(b)], which ultimately overcomes the 25% IQE limit. The RISC efficiency depends on the spin-orbit coupling (SOC) [8–13] and is inversely dependent on the energy difference $\Delta E_{S_1-T_1}$ between S_1 (the lowest singlet state) and T_1 (the lowest triplet state) in the TADF molecule [14–17]. Small $\Delta E_{S_1-T_1}$ values facilitate the thermal up-conversion from T_1 into S_1 [Fig. 1(b)].

As described by the El-Sayed rule [18], the spin mixing between S_1 and T_1 requires a change in the orbital momentum and therefore depends on the SOC strength. In organic materials the SOC is small due to having light elements (such as C, H, O) in their backbone structure, since the SOC depends on Z^4 , where Z is the atomic number. However, the SOC that couples S_1 and T_1 may be enhanced if these states have charge-transfer wave-function characteristics, such as in efficient TADF molecules [9–11].

In 2020, Cui *et al.* [19] and Wada *et al.* [20] reported new TADF molecules with fast RISC rates. With special molecular designs to lower $\Delta E_{S_1-T_1}$ and enhance the SOC of S_1 and T_1 states via charge-transfer characteristics, a fast RISC rate could be realized. For the target material in the present work, 5Cz-TRZ (9,9',9'',9''',9''''-(6-(4,6-diphenyl-1,3,5-triazine-2-yl)benzene-1,2,3,4,5-pentyl)pentakis(9H-carbazole)) [see Fig. 1(a)], $\Delta E_{S_1-T_1}$ is only 0.02 eV; as a result, the RISC rate k_{RISC} in this material was measured to be as fast as $1.5 \times 10^7 \text{ s}^{-1}$ [19]. The fast k_{RISC} was manifested in OLEDs based on this compound having high IQE, high stability, and low roll-off of electroluminescence (EL) at high current density. Thereafter, the class of fast RISC materials has caused great interest in OLED applications [18–23].

Here we have investigated the optical properties of TADF molecules with fast RISC rates, namely

*panxin0922@gmail.com

†o.kwon@samsung.com

‡val@physics.utah.edu

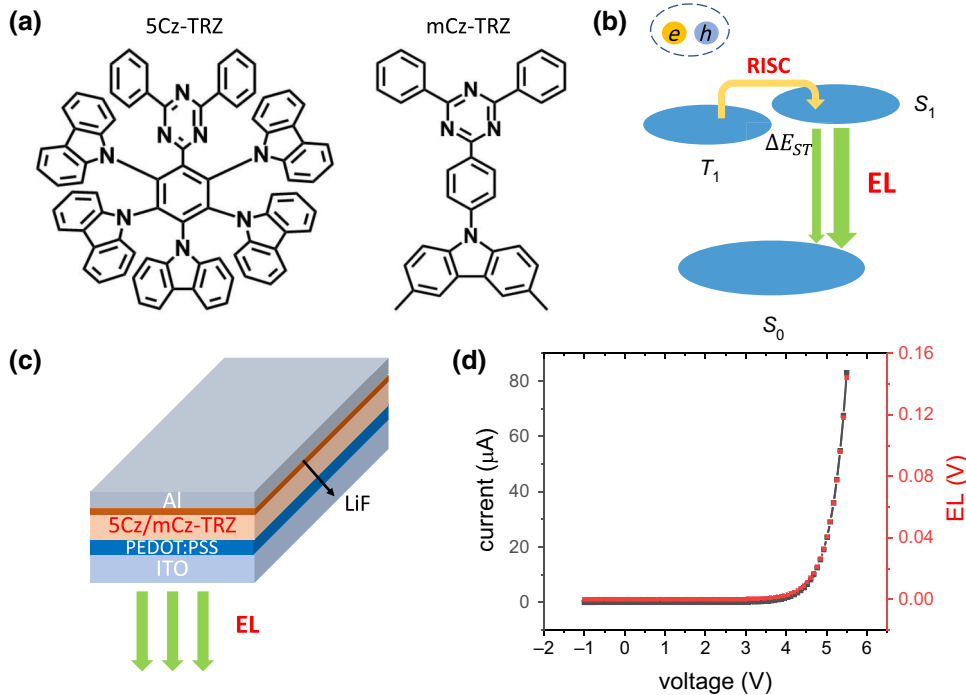


FIG. 1. (a) The molecular structures of the two thermally activated delayed-fluorescence (TADF) materials studied here. (b) Schematic diagram of the reverse intersystem crossing (RISC) process that couples the lowest singlet state S_1 to the lowest triplet state T_1 . Their energy difference $\Delta E_{S_1-T_1}$ is denoted. (c) The organic light-emitting device (OLED) structure based on a 5Cz-TRZ (or mCz-TRZ) emitter layer. (d) Current vs voltage (black squares) and electroluminescence (EL) vs voltage (red squares) in a typical fabricated TADF OLED based on 5Cz-TRZ.

5Cz-TRZ [Fig. 1(a)], and compared them with those of TADF molecules with slow RISC rates, namely mCz-TRZ (9-(4-(4,6-diphenyl-1,3,5-triazin-2-yl)phenyl)-3,6-dimethyl-9H-carbazole) [Fig. 1(a)], using a variety of optical and magneto-optical spectroscopies. In films, we found that the steady-state photoexcitations in 5Cz-TRZ are both triplet and singlet excitons due to the fast RISC rate that mixes these excitations reaching a dynamic equilibrium. However, only triplet excitons have been detected under steady-state illumination conditions in mCz-TRZ films, due to the inefficient RISC process in this compound. In addition, we found that the magnetophotoinduced absorption (MPA) response of the singlet and triplet excitons in films of 5Cz-TRZ are similar and have the same polarity. We therefore conclude that the magnetic field does not have a significant effect on the RISC process in this material.

In traditional TADF OLEDs, the TADF molecules are doped into the host compound to avoid concentration quenching. In this case, the host molecules serve as recombination centers, where the electrons and holes recombine to form excitons that are transferred to the guest molecules [4]. The recombination process is susceptible to the external magnetic field [24]. It is known that the magnetoelectroluminescence (MEL) in exciton-based OLEDs is positive (namely, increases with the magnetic field B) because

the intersystem crossing in the polaron pair (PP) manifold is suppressed by the magnetic field [25]. In contrast, a negative MEL is observed in TADF-based OLEDs because any RISC from charge-transfer states is suppressed by the field, which has been described in Refs. [26–29]. In the present work, we measured the RISC-mediated MEL response in the TADF active materials. Surprisingly, we found that the MEL responses of OLEDs based on the two materials under investigation here are positive, showing no suppression of the RISC-dominated electroluminescence under a magnetic field. This indicates that the magnetic field acts mainly on the injected PP species *before* the excitons are formed in the device active layer. We thus conclude that the magnetic field has little influence on the RISC process in OLEDs based on the studied material, which is therefore dominated by thermal activation rather than by spin dynamics, as previously proposed [28–30].

II. RESULTS AND DISCUSSION

Figure 1(a) shows the molecular structure of the two TADF materials studied here. The five Cz donors in the 5Cz-TRZ molecule lower the S_1 energy level and decrease the $\Delta E_{S_1-T_1}$ value to approximately 20 meV [19]. Since only one Cz donor exists in the mCz-TRZ molecule, $\Delta E_{S_1-T_1}$ is much larger in this compound by of the order of

hundreds of meV [19]; see also Table S1 in the Supplemental Material [44]. The large SOC of the local-excitation-dominated T_1 state and the charge-transfer-dominated S_1 state in 5Cz-TRZ, as well as the small $\Delta E_{S_1-T_1}$, lead to a much faster RISC rate in 5Cz-TRZ than in mCz-TRZ.

We fabricated OLEDs based on the two TADF materials that we purchased from Lumtec Corp. (Taiwan). The device structure is shown in Fig. 1(c) and fabrication details are given in the Experimental Methods section. Typical $I-V$ and EL- V characteristic responses of a 5Cz-TRZ-based OLED are shown in Fig. 1(d). The turn-on voltage of these devices is around 4.5 V with working current as low as 20 μ A. Under low current injection, the diode remains stable with almost constant EL emission intensity for hours.

Next, we discuss the optical characteristic properties of these two molecules both as thin films and as active layers in OLEDs. Figure 2 shows the optical characteristics of 5Cz-TRZ thin films. The absorption spectrum shown in Fig. 2(a) peaks at 3.7 eV, which is at a much higher energy than the S_1 energy (approximately 2.8 eV, see Table S1 in the Supplemental Material [44]). This indicates that the S_1 state has a different symmetry to that of the state responsible for the absorption peak. In fact, the onset of the PL

spectrum seen in Fig. 2(b) is at around 2.8 eV, close to the S_1 energy (see in the Supplemental Material [44]). We thus speculate that S_1 undergoes a substantial relaxation into a charge-transfer state. This may explain the small $\Delta E_{S_1-T_1}$ in this material [19]. We also notice that the PL spectrum shows the 0-1 and 0-2 transition, but not the 0-0 transition [Fig. 2(b)]; this agrees with the lack of direct absorption into the S_1 state seen in Fig. 2(a).

Figure 2(c) shows the steady-state photoinduced absorption (PA) spectrum of the 5Cz-TRZ film. The PA spectrum is composed of two PA bands, one at low energy and one at high energy. The high-energy PA band is due to the S_1-S_2 transition that occurs in the singlet manifold. This PA band was originally discussed by Cui *et al.* [19]. It is formed in the picosecond time domain and has a relatively fast decay, which is characteristic of states in the singlet manifold. We identify the lower-energy PA band, which is much broader, as due to transitions T_1-T_n in the triplet manifold. It has a threshold at a photon energy lower than 0.4 eV, in agreement with the dense triplet manifold (see Table S1 in the Supplemental Material [44]). Furthermore, the MPA response of the lower-energy band [see Fig. 2(d)] is quite broad with features similar to the MPA response of known triplet excitons in π -conjugated polymers, such

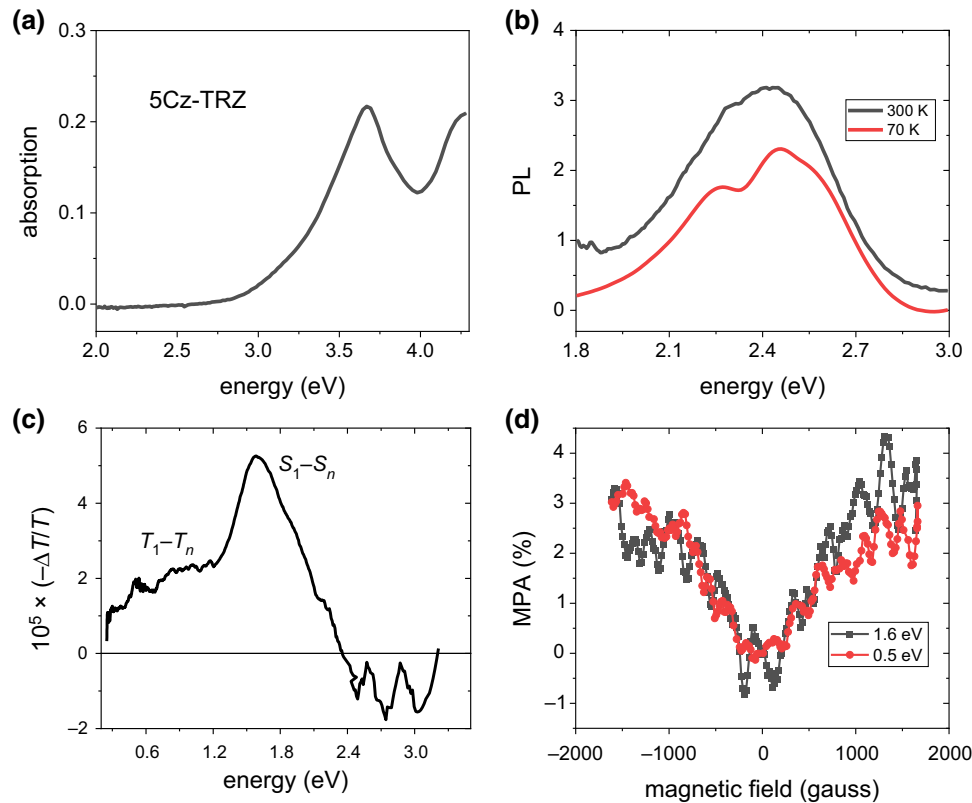


FIG. 2. Optical characterization of 5Cz-TRZ films. (a) The absorption spectrum. (b) The photoluminescence (PL) spectrum of 5Cz-TRZ film measured at room temperature and 70 K. (c) The photoinduced absorption (PA) spectrum measured at 70 K. The PA bands related respectively to optical transitions in the triplet T_1-T_n and singlet S_1-S_n manifolds are assigned. (d) The magnetophotoinduced absorption (MPA) responses at two photon energies related to the two PA bands defined in panel (c).

as MEH-PPV (poly[2-methoxy-5-(2-ethylhexyloxy)-1,4-phenylenevinylene]) [31]. Interestingly, the MPA response of the high-energy PA band is the same as that of the low-energy band and has the same polarity (increasing with the field B). This indicates that under steady-state conditions there is a dynamic equilibrium between S_1 and T_1 due to the fast RISC rate in this compound, such that S_1 “acquires” some properties of T_1 . This does not occur in films of mCz-TRZ, where the RISC rate is much slower, leading to low RISC efficiency, as seen in the following.

In general, the PA bands are related to the photogenerated steady-state triplet-exciton density that is determined by the generation and recombination dynamics. Via the RISC process, the triplet density also determines the steady-state singlet-exciton density. The triplet-exciton species has three spin states that are split by the zero-field-splitting parameters D and E [32]. One of the split triplet states has faster recombination than the two other states, and thus the steady-state population of the two other states is larger. Owing to the applied magnetic field, the three triplet states split further, and this renders the two slower recombination states to be more energetically isolated. Hence their steady-state population increases with the magnetic field. In addition, from the similar polarity of the MPA response for the singlet and triplet excitons, we conclude that the magnetic field has little influence over the RISC process. Otherwise, the MPA responses would have opposite polarities.

In order to compare the influence of the magnetic field on the RISC rate in TADF-based devices, we fabricated OLEDs based on the two studied materials and measured the MEL response, which is defined as $MEL = [\text{EL}_B - \text{EL}_0]/\text{EL}_0$, and can be either positive (enhanced EL intensity) or negative (reduced EL intensity) depending on the dominant spin-related process influenced by the magnetic field. A typical MEL response of a 5Cz-TRZ OLED at room temperature is shown in Fig. 3(a). Since this

MEL(B) response is very different to the MPA(B) response in Fig. 2(d), we conclude that it does not involve the S_1 or T_1 excitons. We thus speculate that the MEL is due to the magnetic field increase of the steady-state injected-PP density in the device active layer *before* forming singlet and triplet excitons.

Our previous work established a method to reveal the relation between the spin pair (here PP) lifetime and the MEL response [33–35]. Most MEL responses in OLEDs are based on spin mixing among the four injected PP spin sublevels, namely one PP singlet (PP_S) and three PP triplet (PP_T) sublevels, which may be provided by several spin-related interactions, such as spin-orbit coupling [36], the hyperfine interaction [36–38], and by the different Landé g values of the electron and hole constituents of the PP species (namely P^- and P^+), commonly known as the “ Δg mechanism” [39].

In the Δg mechanism, the P^- and P^+ spins precess around the magnetic field direction with a precession frequency that is linearly dependent on the magnetic field and the Landé g values of the P^- and P^+ . If $g(P^-) \neq g(P^+)$, and hence $\Delta g = g(P^-) - g(P^+) \neq 0$, then the PP spin configuration interpolates back and forth between the PP_S and PP_T states many times before the steady state is reached. It has been shown that when reaching the steady state, the Δg mechanism leads to a Lorentzian MEL response [40], namely,

$$\text{MEL} = \text{MEL}_{\max} \left[\frac{1}{1 + (B/B_0)^2} - 1 \right], \quad (1)$$

where MEL_{\max} is the maximum MEL amplitude at a large B , and B_0 is the half width at half maximum of the MEL response. For the Δg mechanism, it was shown that $B_0 \sim 1/(\mu_B \Delta g \tau)$, where μ_B is the Bohr magneton and τ is the PP spin or recombination lifetime, whichever is

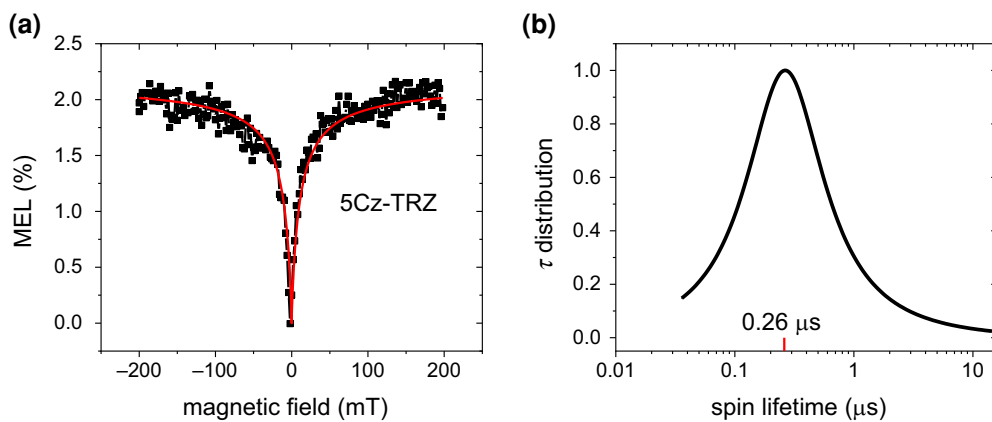


FIG. 3. Magnetoelectroluminescence (MEL) response in the 5Cz-TRZ-based OLED. (a) MEL response at room temperature operated at $20\text{-}\mu\text{A}$ current injection. The red line through the data points is a fit using Eq. (2). (b) The lifetime distribution $g(\tau)$ of the injected polaron pair species extracted from the fit in (a) using Eq. (3).

shorter [40]. However, it is common to measure a non-Lorentzian MEL line shape [34,35] when a broad distribution of relaxation times exists in the organic active-layer materials [41,42]. Equation (1) is written for a single lifetime τ . However, in disordered organic semiconductor deposited films, it is natural to assume that the lifetime of injected PPs is broadly distributed, and thus the “dispersive dynamics” mechanism may dominate the MEL response [23,40]. In this case the broad distribution of lifetime $g(\tau)$ would drastically change the MEL Lorentzian response because each MEL response based on a single lifetime needs to be weighted by the normalized $g(\tau)$ function. A more formal way to account for this type of inhomogeneity is by considering a Cole-Cole function, namely $MEL_{cc} \propto \text{Re}[1/(1 + (iB/B_0)^\alpha)]$, where $\alpha \leq 1$ is a phenomenological “dispersive parameter”.

The Cole-Cole MEL_{cc} dispersive response is a non-Lorentzian function, as follows [43]:

$$MEL_{cc} \propto \left[\frac{1 + (B/B_0)^\alpha \cos(\pi\alpha/2)}{1 + 2(B/B_0)^\alpha \cos(\pi\alpha/2) + (B/B_0)^{2\alpha}} - 1 \right], \quad (2)$$

where the averaged spin or recombination $e\text{-}h$ lifetime τ_0 can be obtained from B_0 using the usual relation mentioned previously, namely $B_0 \sim (\mu_B \Delta g \tau_0)^{-1}$.

A convenient relationship was recently found between the dispersive parameter α , τ_0 , and the lifetime distribution function $g(\tau)$ that gives rise to the MEL_{cc} response, allowing us to obtain the $g(\tau)$ lifetime distribution of the PPs directly from the MEL_{cc} response as follows [43]:

$$g(\ln(\tau/\tau_0)) = \frac{1}{2\pi} \left(\frac{\sin \pi\alpha}{\cosh(\alpha \ln(\tau/\tau_0)) + \cos \pi\alpha} \right). \quad (3)$$

This relation makes it possible to obtain the PP spin lifetime distribution function $g(\tau)$ in the device simply by fitting the measured MEL response using Eq. (2) and subsequently using the parameters α and τ_0 in Eq. (3). This is an elegant, effective, and noninvasive method for obtaining the *in situ* PP lifetime distribution in a working device.

Using the dispersive dynamics method, we fitted the MEL response using Eq. (2) and obtained the PP spin lifetime distribution in the 5Cz-TRZ interlayer film in the device, as shown in Fig. 3(b). The best fitting results give the following parameters: $B_0 = 10.7 \pm 0.6$ mT and $\alpha = 0.68 \pm 0.03$. The mean PP spin lifetime in the device is thus calculated to be 0.26 ± 0.01 μs .

The RISC rate in mCz-TRZ is about 4 orders of magnitude slower than that in 5Cz-TRZ [19], so we expect to see changes in its optical and magneto-optical responses. Figure 4(a) shows the absorption and PL spectra of a pristine mCz-TRZ film. The absorption spectrum is dominated by a band that peaks at around 3.2 eV with a threshold at about 3.0 eV. In contrast to the PL in the 5Cz-TRZ film that shows a substantial Stokes shift [Fig. 2(b)], the PL in

the mCz-TRZ film shows a relatively small Stokes shift, since the threshold energy in the PL spectrum is at about 3.0 eV, which coincides with that of the absorption-band threshold. This shows that S_1 here is optically active and does not undergo large relaxation and coordinate change into the charge-transfer state that occurs in 5Cz-TRZ. This also explains the large $\Delta E_{S_1-T_1}$ in this compound, which renders RISC less plausible. We thus expect that the triplet exciton in mCz-TRZ is more stable than in 5Cz-TRZ.

Figure 4(b) shows the PA spectrum in the mCz-TRZ film. The spectrum shows a single PA band that extends over the measured spectral range, with a threshold at approximately 0.4 eV. The calculated energy difference $\Delta E_{T_3-T_1}$ between the T_3 and T_1 states in the triplet manifold is approximately 0.45 eV (see Table S1 in the Supplemental Material [44]), which is in agreement with the threshold energy of the PA band here. We thus assign this PA as being due to the $T_1\text{-}T_n$ transition in the triplet manifold. Importantly, the high-energy PA band due to the singlet exciton that dominates the PA spectrum in 5Cz-TRZ is *absent* in mCz-TRZ. This indicates that the photogenerated singlet exciton undergoes intersystem crossing into the triplet manifold and rarely participates in an eventual RISC process. The acute difference between the PA spectra of the two TADF compounds studied here is clearly in agreement with their vastly different RISC dynamics that are dominated by the difference in their $\Delta E_{S_1-T_1}$ values.

The MEL response of mCz-TRZ based OLED is shown in Fig. 4(c). Compared with the 5Cz-TRZ-based OLED, the threshold current density for observing EL here is much larger [by at least 2 orders of magnitude (see Fig. S2 in the Supplemental Material [44]). Surprisingly, the MEL response of the mCz-TRZ-based OLED [Fig. 4(c)] is very similar to that of the 5Cz-TRZ-based OLED [Fig. 3(a)]. Additionally, the positive MEL response indicates that the magnetic field enhances the EL intensity here and, according to the literature, it is not due to the field influence of the RISC process [24–26]. Using the same analysis of this MEL response as performed for the MEL response for the 5Cz-TRZ-based OLED described previously, we obtain the following parameters: $B_0 = 7.2 \pm 0.4$ mT and $\alpha = 0.86 \pm 0.03$. The mean PP spin lifetime in mCz-TRZ is calculated to be 0.39 ± 0.02 μs , which is comparable to that in the 5Cz-TRZ-based OLED. The short lifetime cannot be related to the RISC process, since it is very slow in mCz-TRZ. This indicates that the obtained lifetime is due to the injected PP species rather than the excitons in this compound, in agreement with our conclusion for the 5Cz-TRZ-based OLED discussed previously.

In addition, from the similar MEL response in the two OLEDs based on the fast and slow RISC rates, we conclude that the MEL is dominated by the PP species. Since the RISC-related MEL is negative, whereas the PP-related MEL is positive, we would have seen a sign change in the MEL response, especially in the 5Cz-TRZ-based OLED.

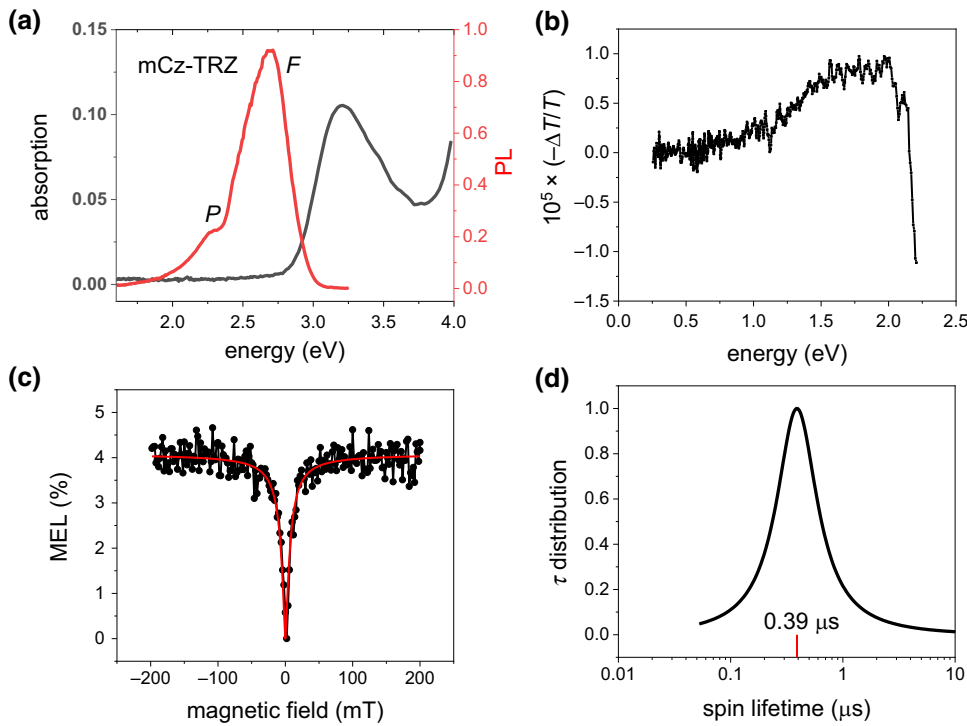


FIG. 4. Optical and magneto-optical properties of mCz-TRZ. (a) The absorption and photoluminescence (PL) spectra of mCz-TRZ thin film measured at room temperature. F denotes fluorescence; P denotes phosphorescence. (b) The photoinduced absorption spectrum due to optical transitions T_1-T_n in the triplet manifold. (c) The magnetooptical luminescence (MEL) response of a mCz-TRZ-based organic light-emitting device measured at room temperature at 3-mA current injection. The red line through the data points is a fit using Eq. (2). (d) The lifetime distribution $g(\tau)$ of the injected polaron pair species in the device extracted from the fit in (c) using Eq. (3).

The fact that we do not detect such a sign change in the MEL response strongly indicates that the applied field does not influence the RISC process in the studied TADF materials here.

III. CONCLUSION

We have studied the optical and magneto-optical properties of 5Cz-TRZ and mCz-TRZ in thin-film and OLED configurations. We have shown that their optical properties are dominated by their $\Delta E_{S_1-T_1}$ value, which is much larger in mCz-TRZ than in 5Cz-TRZ. The RISC process in 5Cz-TRZ is fast and effective, and this leads to a much larger EL quantum efficiency. Additionally, the steady-state PA shows two PA bands that are due to photoinduced transitions in the singlet and triplet manifolds, because of the fast dynamic equilibrium that is established between the singlet and triplet excitons in this compound. From the similar polarity of the MPA response for the singlet and triplet excitons, we conclude that the field has little influence on the RISC process in this compound. In contrast, the PA of the mCz-TRZ film shows only photoinduced transitions in the triplet manifold since the RISC process is less effective in this compound. Surprisingly the MEL response in OLEDs based on these two TADF molecules

is positive, which is opposite to the RISC-mediated MEL response due to suppression of the RISC process under a magnetic field. This shows that the magnetic field influences the injected PP species *before* excitons are formed in the TADF material.

IV. EXPERIMENTAL METHODS

A. Device engineering

The OLEDs were composed of a patterned indium tin oxide (ITO)-coated glass; an approximately 30-nm-thick hole transport layer, namely poly(3,4-ethylenedioxythiophene) polystyrene sulphonate (PEDOT:PSS); the active layer (TADF molecules); an electron transport layer (PCBM, phenyl-C₆₁-butyric acid methyl ester); a buffer layer (LiF); and capped with an Al electrode [see Fig. 1(c)]. The OLED devices were fabricated on a patterned ITO-coated glass ($15\text{--}20 \Omega \text{ cm}^{-2}$; Luminescence Tech.). We precleaned the ITO-coated glass substrates sequentially with deionized water (DI water, 200 ml) with 2% micro-90 soap, pure DI water (200 ml), acetone (100 ml), and isopropanol (100 ml) for 15 min by means of an ultrasonic bath. Subsequently the substrates were dried by nitrogen blow and treated with ultraviolet ozone for 8 min.

We deposited an approximately 30-nm-thick hole transport layer (PEDOT:PSS, Clevios P VP AI 4083) that was annealed in air for 20 min at 140 °C.

We used the 5Cz-TRZ and mCz-TRZ as the active emitting layers [see Fig. 1(a)]. 5Cz-TRZ and mCz-TRZ were purchased from Lumtec Corp. (Taiwan) and used without further purification. A layer of an approximately 80-nm-thick film of TADF molecules was thermally deposited. The OLED devices were then capped with a LiF(1 nm)/Al(100 nm) electrode that was thermally evaporated through a shadow mask that defined an active area of around 4 mm².

B. MEL measurements

For the MEL measurements, the OLED devices were transferred into a cryostat that was placed between the poles of an electromagnet that produced an in-plane magnetic field **B** with field strength *B* up to 200 mT. The MEL measurements were performed in the cryostat at room temperature. The *I-V* characteristic response was obtained using a standard “four points” method with a Keithley 236 power supply and Keithley-2000 multimeter. The EL and MEL measurements were performed at constant current density *J*. To avoid possible interference with the magnetoconductivity of the wires, we used electrical wires made of metallic alloys to keep the parasitic magnetoresistance below 0.001%. The EL emission was monitored using a silicon detector. The OLED devices were operated at a forward bias $V_b > V_{th}$, where V_{th} is the threshold bias voltage for the EL, while sweeping the external magnetic field in one direction and back for several cycles to improve the SNR ratio. The MEL is defined as $MEL = EL_B/EL_0 - 1$] measured under constant current condition.

C. Photoinduced absorption measurements

The PA spectra were measured by a cw “pump probe” set up in the spectral range from 450 nm to 5 μm using several solid-state detectors, such as Si, Ge, and InSb. The “pump” was a laser diode operating at 3.4 eV, which was modulated at 150 Hz using a chopper controlled by a function generator. The “probe” was light coming from a tungsten-halogen incandescent lamp that was dispersed by a ¼-m monochromator. The change ΔT in the probe transmission spectrum *T* induced by the pump-beam excitation was monitored using a lock-in amplifier referenced to the pump-beam modulation. The PA spectrum was subsequently calculated as $-\Delta T/T$. For the MPA measurements, thin films were transferred into a cryostat that was placed in an in-plane magnetic field **B** with field strength *B* up to 200 mT.

D. Energy-level calculations

To obtain the energy levels for Table S1 in the Supplemental Material [44], the molecular structures of 5Cz-TRZ

and mCz-TRZ were fully optimized at the B3LYP/6-31G** level. Excited states of the molecules were then calculated at the TD-B3LYP/6-31G** level in the time-dependent density-functional-theory formalism based on the optimized geometries.

ACKNOWLEDGMENTS

This work was supported by the SAMSUNG Global Research Outreach (GRO) program (X.P. and the MEL studies); and by the DOE, Office of Science, Grant No. DE-SC0014579 (D.R.K and the PA studies).

- [1] Ayataka Endo, Keigo Sato, Kazuaki Yoshimura, Takahiro Kai, Atsushi Kawada, Hiroshi Miyazaki, and Chihaya Adachi, Efficient up-conversion of triplet excitons into a singlet state and its application for organic light emitting diodes, *Appl. Phys. Lett.* **98**, 8 (2011).
- [2] Qisheng Zhang, Bo Li, Shuping Huang, Hiroko Nomura, Hiroyuki Tanaka, and Chihaya Adachi, Efficient blue organic light-emitting diodes employing thermally activated delayed fluorescence, *Nat. Photonics* **8**, 326 (2014).
- [3] Shuzo Hirata, Yumi Sakai, Kensuke Masui, Hiroyuki Tanaka, Sae Youn Lee, Hiroko Nomura, Nozomi Nakamura, *et al.*, Highly efficient blue electroluminescence based on thermally activated delayed fluorescence, *Nat. Mater.* **14**, 330 (2015).
- [4] Hiroki Uoyama, Kenichi Goushi, Katsuyuki Shizu, Hiroko Nomura, and Chihaya Adachi, Highly efficient organic light-emitting diodes from delayed fluorescence, *Nature* **492**, 234 (2012).
- [5] Katsuaki Suzuki, Shosei Kubo, Katsuyuki Shizu, Tatsuya Fukushima, Atsushi Wakamiya, Yasujiro Murata, Chihaya Adachi, and Hironori Kaji, Triarylboron-based fluorescent organic light-emitting diodes with external quantum efficiencies exceeding 20%, *Angew. Chem., Int. Ed.* **127**, 15446 (2015).
- [6] Naoya Aizawa, Yong-Jin Pu, Yu Harabuchi, Atsuko Nihonyanagi, Ryotaro Ibuka, Hiroyuki Inuzuka, Barun Dhara, *et al.*, Delayed fluorescence from inverted singlet and triplet excited states, *Nature* **609**, 502 (2022).
- [7] Hajime Nakanotani, Youichi Tsuchiya, and Chihaya Adachi, Thermally-activated delayed fluorescence for light-emitting devices, *Chem. Lett.* **50**, 938 (2021).
- [8] Xian-Kai Chen, Shou-Feng Zhang, Jian-Xun Fan, and Ai-Min Ren, Nature of highly efficient thermally activated delayed fluorescence in organic light-emitting diode emitters: nonadiabatic effect between excited states, *J. Phys. Chem. C* **119**, 9728 (2015).
- [9] Jamie Gibson, Andrew P. Monkman, and Thomas J. Penfold, The importance of vibronic coupling for efficient reverse intersystem crossing in thermally activated delayed fluorescence molecules, *ChemPhysChem* **17**, 2956 (2016).
- [10] Fernando B. Dias, Jose Santos, David R. Graves, Przemyslaw Data, Roberto S. Nobuyasu, Mark A. Fox, Andrei S. Batsanov, *et al.*, The role of local triplet excited states and

- D-A relative orientation in thermally activated delayed fluorescence: Photophysics and devices, *Adv. Sci.* **3**, 1600080 (2016).
- [11] Christel M. Marian, Mechanism of the triplet-to-singlet upconversion in the assistant dopant ACRXTN, *J. Phys. Chem. C* **120**, 3715 (2016).
- [12] Takuya Hosokai, Hiroyuki Matsuzaki, Hajime Nakano-tani, Katsumi Tokumaru, Tetsuo Tsutsui, Akihiro Furube, Keirou Nasu, Hiroko Nomura, Masayuki Yahiro, and Chihaya Adachi, Evidence and mechanism of efficient thermally activated delayed fluorescence promoted by delocalized excited states, *Sci. Adv.* **3**, e1603282 (2017).
- [13] J. Gibson and T. J. Penfold, Nonadiabatic coupling reduces the activation energy in thermally activated delayed fluorescence, *Phys. Chem. Chem. Phys.* **19**, 8428 (2017).
- [14] Nicholas J. Turro, Vaidhyanathan Ramamurthy, and Juan C. Scaiano, *Principles of Molecular Photochemistry: An Introduction* (University science books, New York, 2009).
- [15] Jean-Luc Brédas, David Beljonne, Veaceslav Coropceanu, and Jérôme Cornil, Charge-transfer and energy-transfer processes in π -conjugated oligomers and polymers: A molecular picture, *Chem. Rev.* **104**, 4971 (2004).
- [16] Pralok K. Samanta, Dongwook Kim, Veaceslav Coropceanu, and Jean-Luc Brédas, Up-conversion intersystem crossing rates in organic emitters for thermally activated delayed fluorescence: impact of the nature of singlet vs triplet excited states, *J. Am. Chem. Soc.* **139**, 4042 (2017).
- [17] Marc K. Etherington, Jamie Gibson, Heather F. Higginbotham, Thomas J. Penfold, and Andrew P. Monkman, Revealing the spin–vibronic coupling mechanism of thermally activated delayed fluorescence, *Nat. Commun.* **7**, 13680 (2016).
- [18] M. A. El-Sayed, Spin–orbit coupling and the radiationless processes in nitrogen heterocyclics, *J. Chem. Phys.* **38**, 2834 (1963).
- [19] Lin-Song Cui, Alexander J. Gillett, Shou-Feng Zhang, Hao Ye, Yuan Liu, Xian-Kai Chen, Ze-Sen Lin, *et al.*, Fast spin-flip enables efficient and stable organic electroluminescence from charge-transfer states, *Nat. Photonics* **14**, 636 (2020).
- [20] Yoshimasa Wada, Hiromichi Nakagawa, Soma Matsumoto, Yasuaki Wakisaka, and Hironori Kaji, Organic light emitters exhibiting very fast reverse intersystem crossing, *Nat. Photonics* **14**, 643 (2020).
- [21] Kenkera Rayappa Naveen, Paramasivam Palanisamy, Mi Young Chae, and Jang Hyuk Kwon, Multiresonant TADF materials: Triggering the reverse intersystem crossing to alleviate the efficiency roll-off in OLEDs, *Chem. Commun.* **59**, 3685 (2023).
- [22] Thanh-Tuân Bui, Fabrice Goubard, Malika Ibrahim-Ouali, Didier Gigmes, and Frédéric Dumur, Recent advances on organic blue thermally activated delayed fluorescence (TADF) emitters for organic light-emitting diodes (OLEDs), *Beilstein J. Org. Chem.* **14**, 282 (2018).
- [23] Dehua Hu, Liang Yao, Bing Yang, and Yuguang Ma, Reverse intersystem crossing from upper triplet levels to excited singlet: A ‘hot excitation’ path for organic light-emitting diodes, *Philos. Trans. R. Soc., A* **373**, 20140318 (2015).
- [24] Junquan Deng, Weiyao Jia, Yingbing Chen, Dongyu Liu, Yeqian Hu, and Zuhong Xiong, Guest concentration, bias current, and temperature-dependent sign inversion of magneto-electroluminescence in thermally activated delayed fluorescence devices, *Sci. Rep.* **7**, 44396 (2017).
- [25] Bin Hu, Liang Yan, and Ming Shao, Magnetic-field effects in organic semiconducting materials and devices, *Adv. Mater.* **21**, 1500 (2009).
- [26] Ping Chen, Zuhong Xiong, Qiming Peng, Jiangwen Bai, Shitong Zhang, and Feng Li, Magneto-electroluminescence as a tool to discern the origin of delayed fluorescence: Reverse intersystem crossing or triplet–triplet annihilation?, *Adv. Opt. Mater.* **2**, 142 (2014).
- [27] Ping Chen, Li-Ping Wang, Wan-Yi Tan, Qi-Ming Peng, Shi-Tong Zhang, Xu-Hui Zhu, and Feng Li, Delayed fluorescence in a solution-processable pure red molecular organic emitter based on dithienylbenzothiadiazole: A joint optical, electroluminescence, and magnetoelectroluminescence study, *ACS Appl. Mater. Interfaces* **7**, 2972 (2015).
- [28] Qiming Peng, Aiwu Li, Yunxia Fan, Ping Chen, and Feng Li, Studying the influence of triplet deactivation on the singlet–triplet inter-conversion in intra-molecular charge-transfer fluorescence-based OLEDs by magneto-electroluminescence, *J. Mater. Chem. C* **2**, 6264 (2014).
- [29] Qiming Peng, Weijun Li, Shitong Zhang, Ping Chen, Feng Li, and Yuguang Ma, Evidence of the reverse intersystem crossing in intra-molecular charge-transfer fluorescence-based organic light-emitting devices through magneto-electroluminescence measurements, *Adv. Opt. Mater.* **1**, 362 (2013).
- [30] Xi Zhao, Xiantong Tang, Ruiheng Pan, Jing Xu, Fenlan Qu, and Zuhong Xiong, Direct observation of reverse intersystem crossing from fully confined triplet exciplexes using magneto-electroluminescence, *J. Mater. Chem. C* **7**, 10841 (2019).
- [31] Bhoj R. Gautam, Tho D. Nguyen, Eitan Ehrenfreund, and Zeev Valy Vardeny, Magnetic field effect on excited-state spectroscopies of π -conjugated polymer films, *Phys. Rev. B* **85**, 205207 (2012).
- [32] *Handbook of Conducting Polymers*, 4th ed., edited by J. R. Reynolds, B. C. Thompson, and T. A. Skotheim (CRC Press/Taylor & Francis, Boca Raton, 2019).
- [33] Ryan McLaughlin, Xin Pan, Dali Sun, Ohyun Kwon, and Zeev Valy Vardeny, Study of photocarriers lifetime distribution in a-Si:H via magneto-photoconductivity and magneto-photoluminescence, *Adv. Opt. Mater.* **10**, 2200499 (2022).
- [34] Amit Kumar Mondal, Xin Pan, Ohyun Kwon, and Zeev Valy Vardeny, Degradation analysis of organic light-emitting diodes through dispersive magneto-electroluminescence response, *ACS Appl. Mater. Interfaces* **15**, 9697 (2023).
- [35] Xin Pan, Ohyun Kwon, Dipak Raj Khanal, Byoungki Choi, and Zeev Valy Vardeny, Disorder-induced dispersive magneto-electroluminescence of blue emitters in organic light emitting diodes, *Adv. Opt. Mater.* **10**, 2101334 (2022).

- [36] James Rybicki, Tho Duc Nguyen, Yugang Sheng, and Markus Wohlgemann, Spin-orbit coupling and spin relaxation rate in singly charged π -conjugated polymer chains, *Synth. Met.* **160**, 280 (2010).
- [37] T. D. Nguyen, B. R. Gautam, E. Ehrenfreund, and Z. Valy Vardeny, Magnetoconductance response in unipolar and bipolar organic diodes at ultrasmall fields, *Phys. Rev. Lett.* **105**, 166804 (2010).
- [38] Tho D. Nguyen, Golda Hukic-Markosian, Fujian Wang, Leonard Wojcik, Xiao-Guang Li, Eitan Ehrenfreund, and Z. Valy Vardeny, Isotope effect in spin response of π -conjugated polymer films and devices, *Nat. Mater.* **9**, 345 (2010).
- [39] C. Zhang, D. Sun, C. X. Sheng, Y. X. Zhai, K. Mielczarek, A. Zakhidov, and Z. V. Vardeny, Magnetic field effects in hybrid perovskite devices, *Nat. Phys.* **11**, 427 (2015).
- [40] Ayeleth H. Devir-Wolfman, Bagrat Khachatrian, Bhoj R. Gautam, Lior Tzabary, Amit Keren, Nir Tessler, Z. Valy Vardeny, and Eitan Ehrenfreund, Short-lived charge-transfer excitons in organic photovoltaic cells studied by high-field magneto-photocurrent, *Nat. Commun.* **5**, 4529 (2014).
- [41] O. Epshtain, G. Nakhmanovich, Y. Eichen, and E. Ehrenfreund, Dispersive dynamics of photoexcitations in conjugated polymers measured by photomodulation spectroscopy, *Phys. Rev. B* **63**, 125206 (2001).
- [42] A. Bello, E. Laredo, and M. Grima, Distribution of relaxation times from dielectric spectroscopy using Monte Carlo simulated annealing: Application to α -PVDF, *Phys. Rev. B* **60**, 12764 (1999).
- [43] Kenneth S. Cole and Robert H. Cole, Dispersion and absorption in dielectrics I. Alternating current characteristics, *J. Chem. Phys.* **9**, 341 (1941).
- [44] See Supplemental Material at <http://link.aps.org/supplemental/10.1103/PhysRevApplied.21.034057> for Figs. S1–S2 and Table S1. Supplemental Material is available free of charge at AOM. Data related to current dependence of MEL(B) response in 5Cz-TRZ OLEDs; I-V characteristics in mCz-TRZ OLEDs; calculated energy levels in 5Cz-TRZ and mCz-TRZ molecules.